Central European Geology, Vol. 60/2, 152–172 (2017)
DOI: 10.1556/24.60.2017.006
First published online June 19, 2017

Preliminary fluid inclusion microthermometry results from secondary inclusion planes crosscutting a metamorphic quartz lens from the Mecsekalja Zone metamorphic complex

Gergely Dabi[1]*, Ferenc Tóth[2], Félix Schubert[1]

[1]Department of Mineralogy, Geochemistry and Petrology, University of Szeged, Szeged, Hungary
[2]Békés Drén – Environmental, Water and Civil Engineering Ltd., Békés, Hungary

Received: September 27, 2016; accepted: March 1, 2017

In this study, new microthermometric data of fluid inclusions distributed along planar assemblages crosscutting a metamorphic quartz lens from the Mecsekalja Zone metamorphic complex are presented. Three fluid generations are defined, none of which have previously been identified by earlier paleofluid evaluations of the study area. Petrographic description of the host quartz is provided to identify textures related to crystalloplastic deformation resulting from ductile deformation. The textural relationship of the studied assemblages to the dynamic recrystallization features is discussed. The possible affinities of the fluids introduced in this study to those identified in the region by previous authors are discussed. The affinities and timing of the fluid flow events are discussed based on the physicochemical properties of the fluids. One local carbonic (high X_{CO2}) fluid is recognized. A high- and a moderate-salinity fluid generation are also revealed. The relationship of these fluid generations to those defined in earlier studies from the Mórágy Granite and the Baksa metamorphic complex contributes new knowledge to the recognition of the regional paleofluid evolution.

Keywords: paleofluid, fluid inclusion, CO_2 inclusions, metamorphic quartz, Mecsekalja Zone

*Corresponding author: Gergely Dabi; Department of Mineralogy, Geochemistry and Petrology, University of Szeged, Egyetem u. 2, H-6722 Szeged, Hungary
E-mail: gergely.dabi@gmail.com

This is an open-access article distributed under the terms of the Creative Commons Attribution License, which permits unrestricted use, distribution, and reproduction in any medium for non-commercial purposes, provided the original author and source are credited.

ISSN 1788-2281 © 2017 *The Author(s)*

Introduction

Fluid inclusion planes (FIPs) are fossilized mode I microcracks, formed perpendicular to the σ_3 direction in minerals, which can be mechanically considered isotropic during brittle deformation, e.g., in quartz (Lespinasse 1999). The microcracks heal imperfectly due to the redistribution of SiO_2 inside the microcrack fluid, leaving behind planar assemblages of fluid inclusions filled with the fluid present in the rock contemporaneously with the deformation event. The presence of FIPs is thus the evidence of the pervasion of crustal fluids along microcrack systems in crystalline rocks during tectonic loading. Rock mechanics suggest that the opening of the mode I microcracks precursory to FIPs antedates the opening of transgranular microcracks, e.g., wing cracks, during a loading cycle (Paterson and Wong 2005). The systematic spatial distribution of FIP orientations and densities around faults evince that their formation is related to fault action (Faulkner et al. 2006; Mitchell and Faulkner 2009, 2012). On the whole, FIPs provide an invaluable source of information of fluid-rock interaction during deformation in the brittle regime.

The recognition of paleofluid evolution of the Mecsekalja Zone (MZ) metamorphic complex is based on the crosscutting vein systems and their fluid inclusion assemblages (Dabi et al. 2009, 2011, 2013), whereas that of the Mórágy Granite is based on both the investigation of veins hosted in the granitic rocks (and related fluid inclusion assemblages; Szabó et al. 2003; Poros et al. 2008) and the petrography and microthermometry of FIPs of the rock-forming quartz (Poros et al. 2008; Szabó et al. 2008). The paleofluid evolution of the MZ and the Mórágy Granite has several common features (e.g., Dabi et al. 2011). The fluid evolution of the MZ is based on crosscutting vein systems, which are representative of fracture-channelized flow events in the geologic past. This study is a venture to reveal the suitability of rock-forming quartz veins for the investigation of crosscutting fluid inclusion assemblages. Our preliminary petrographic and microthermometric data prove that the fluid inclusion assemblages crosscutting the rock-forming metamorphic quartz lenses of the MZ metamorphic complex contain a wealth of undiscovered information that can contribute to the recognition of the paleofluid evolution of the MZ and its surroundings. However, difficulties and limitations of fluid inclusion petrography are also recognized, due to the recrystallization of the studied sample inherited from mylonitization, which is probably ubiquitous in the study area.

Geologic background

MZ (Ófalu Group)

The MZ is a ca. 1.5-km-wide, NE–SW trending fault zone located in the Eastern Mecsek Mountains, Hungary (Fig. 1A and B), which can be traced in boreholes to the northeast and the southwest beneath a thick cover of overlying Cenozoic to quaternary

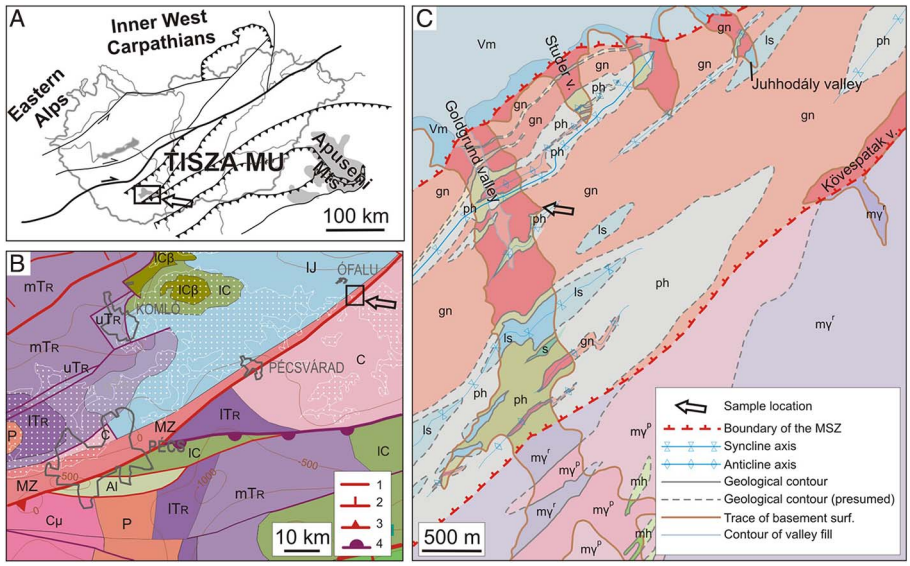

Fig. 1
Geologic background. (A) Position of the Tisza Mega-unit in the basement of the Pannonian Basin. Inset shows the position of B. (B) Regional geologic map of the study area. The MZ is a narrow metamorphic zone between Mesozoic sequences in the Eastern Mecsek Mountains and the Variscan Mórágy Granite, Mórágy Hills. The contact of the MZ is tectonic both to the north and to the south. Dotted area marks surface outcrops of the pre-Cenozoic formations. (1) Cenozoic tectonic line, (2) Cenozoic fault, (3) Cenozoic overthrust, and (4) Mesozoic nappe. Inset shows the position of C. (C) Outcrops of the MZ are exposed in the north–south valleys southeast of the village of Ófalu. MZ, Mecsekalja Zone; C, Variscan granitoid rocks; P, Permian; lTR, Lower Triassic; mTR, Middle Triassic; uTR, Upper Triassic to Lower Jurassic; lJ, Lower to Middle Jurassic; lC, Upper Jurassic to Lower Cretaceous; lCβ, Lower Cretaceous basaltic rocks; Al, Albian; gn, gneiss; ph, phyllite; s, serpentinite; ls, limestone; $m\gamma^r$, rarely porphyritic monzogranite; $m\gamma^p$, porphyritic monzogranite; mh, monzonite; Vm, Vasas Marl Formation. After Balla et al. (2009)

sediments. The northern boundary of the MZ is the so-called Ófalu Fault (Balla et al. 2009), which separates Jurassic marls (Vasas Marl Formation) from the Variscan metamorphic crystalline complex (Fig. 1C). The strike of the boundary changes between NE–SW and ENE–WSW in the study area, the dip angle of the fault is 50° toward NW according to coal exploration boreholes in the northern surroundings (Gulácsi and Koroknai 2009). Full knowledge of the history of the Ófalu Fault in the geologic past is still unknown due to poor outcropping (Balla et al. 2009). At present, the most plausible interpretation is that the Ófalu Fault is a normal fault formed after the Early Cretaceous, according to the age of the footwall and the hanging wall rocks, and the continuity of the Jurassic–Early Cretaceous sequence in the Mecsek Mountains (Balla et al. 2009). From the southeastern boundary to the rocks of the Mórágy Granite Formation, thick fracture zones are described by previous authors, but parallel mylonitic foliation of the MZ metamorphic rocks and the Mórágy Granite indicate

their shared tectonic history since the Variscan (Koroknai 2009a). The MZ includes a very heterogeneous metamorphic rock assemblage; knowledge of the internal structure (Fig. 1C) has a considerable degree of uncertainty due to poor outcrop conditions and reflects the approximate quantitative relationships of the main rock types (Koroknai 2009a). The most prevalent rocks are mylonitized gneisses, which enclose outcrop- to map-scale elongated, lens-shaped bodies of amphibolite, serpentinite and marble (Fig. 1C). According to Koroknai (2009a), the southern part is mainly composed of metamorphic rocks of sedimentary origin (including the crystalline limestone body; Fig. 1C) with phyllonite as the enclosing "matrix" of the lens-like rock bodies. The gneisses of the northern part are of magmatic origin, based on zircon morphology (M. Tóth et al. 2005). Rocks are grouped into different types, i.e., biotite gneiss, banded gneiss, augengneiss, white gneiss, and phyllonite (Gulácsi and Koroknai 2009). The gneissic rocks display intense folding and mylonitization at greenschist facies (M. Tóth et al. 2005). These types are basically different in their texture and their mineralogical compositions are very diverse, even within the same type. Textural evidence of mylonitic shear is obvious throughout the MZ; mica fishes, "V"-pull parts of feldspars, dynamically recrystallized quartz ribbons, and seams are ubiquitous in thin section. The age of the mylonitic deformation has been dated to between 303 and 270 Ma with the Ar–Ar method (Lelkes-Felvári et al. 2000). Based on zircon morphology, the precursory rock of the mylonite has been defined as orthogneiss, the protolith of which crystallized at 710 °C followed by metamorphic recrystallization at 550 °C (M. Tóth et al. 2005).

The brittle structural evolution of the MZ is scarcely known due to the poor exposure of the rocks. The similar orientation of the mylonitic foliation of the MZ metamorphic rocks and the mylonitic foliation of the Mórágy Granite suggest their common structural evolution since the Late Carboniferous–Early Permian. The fault structure inside the Mórágy Granitoid Complex is precisely recognized due to the very detailed investigation in the past 20 years aiming at the final deposition of low- and intermediate-level radioactive waste, and during the implementation of two inclined shafts to the deposition chambers (Maros et al. 2004, 2009).

Paleohydrogeologic evolution of the MZ

Dabi et al. (2011) studied the paleohydrogeologic evolution of the MZ as it can be reconstructed by the crosscutting vein systems in the Ófalu study area. Based on detailed textural analysis, fluid inclusion microthermometry and stable isotope compositions, the defined vein generations were formed in the period between the Triassic start of carbonaceous sedimentation and the Early Cretaceous volcanic activity in the region. The Early Cretaceous volcanic activity in the region was accompanied by magmatic dike emplacement both in the MZ and the Mórágy Granite to the southeast. A pervasive microcrack generation is prevalent in the MZ metamorphic rocks, the parent fluid of which is related to the dike emplacement, according to its stable isotope compositions (Dabi et al. 2013). This microcrack system is

interpreted to be the fossilized analogue of short-lived damage zones detected in the surroundings of recently active faults (Dabi et al. 2013). The youngest vein generation is an antitaxial crack-seal vein system partially filled with limonite-stained calcite. At some places, syntaxial counterparts of this vein generation have also been found (Dabi et al. 2011). According to stable isotope compositions of the two textural types, its individual veins belong to a single generation (Dabi et al. 2011). Based on the direct contact between the Cretaceous dykes and the limonitic calcite in the Mórágy Granite to the southeast (Koroknai 2009b), the antitaxial crack-seal veins are related to the magmatic volatiles released from the dike material during its crystallization.

Methods

The fluid inclusion studies were carried out at the Department of Mineralogy, Geochemistry and Petrology, University of Szeged, on a Linkam THMSG600 heating–freezing stage mounted on an Olympus BX41 microscope. Doubly polished, 60- to 70-μm-thick chips of the rock-forming quartz lenses were first mapped for fluid inclusions. Final melting temperature measurements were undertaken using the cycling technique (Goldstein and Reynolds 1994). Calibration of the heating–freezing stage was carried out using synthetic inclusions of pure H_2O [T_m(ice) = 0 °C, T_h(crit) = 374 °C] and H_2O–CO_2 inclusions [$T_m(CO_2)$ = 56.6 °C] entrapped in quartz.

Scanning electron microscope (SEM)-based cathodoluminescent (CL) images were taken with a Gatan MiniCL system detector, mounted on a Hitachi S-4700 Type II high-resolution cold cathode field emission SEM at 20 keV accelerating voltage, at the Faculty of Science and Informatics, University of Szeged.

Raman spectroscopy was performed at the Department of Mineralogy, Geochemistry and Petrology, University of Szeged on a Thermo Scientific DXR Raman microscope equipped with a diode-pumped frequency-doubled Nd-YAG laser at 10 mW maximum laser power. The samples were irradiated by laser light at a wavelength of 532.2 nm, with the laser beam focused using a 100× objective lens, resulting in a spot size of ca. 0.7 μm. The backscattered light collected by the microscope objective was filtered through an edge filter, dispersed by a single grating (900 grooves mm^{-1}), and gathered in a CCD detector cooled to −20 °C by the Peltier effect. The instrument had a spectral resolution better than 4 cm^{-1} and a spatial resolution of a few μm^3; a 50 μm pinhole confocal aperture was used for each measurement. In every case, 10 mW laser power was used to record the spectra.

Results

One metamorphic quartz lens was collected at the northern part of the Goldgrund valley near the village of Ófalu (Fig. 1C). The host rock of the studied sample is a greenish micaceous gneiss, most probably belonging to the “biotite gneiss” member of

the "Studervölgy Gneiss Formation" [not yet approved formation classification, proposed by Gulácsi and Koroknai (2009)]. The host rock has a homogeneous greenish macroscopic appearance with schistose foliation and sparse elongated feldspar porphyroclasts. The elongated quartz lenses of maximum 1 cm width parallel to foliation also occur sparsely in the biotite gneiss.

Microscopic description of the studied quartz lenses

One thick section was prepared from the collected sample, perpendicular to the lens. The sample was not oriented. The section was prepared with the aim to study the petrography of the crosscutting FIPs, and to carry out fluid inclusion microthermometry; thus the optical properties of the section are somewhat discrepant from those of a standard thin section: the optical discrepancies take shape in higher interference colors. Nevertheless, the textural features could be successfully defined and set against the features discussed in the appropriate literature on quartz recrystallization (for a detailed summary, see Tullis et al. 2000; Passchier and Trouw 2005).

The quartz lens displays heterogeneous deformation, with domains of different recrystallization features (Fig. 2). The transition from domains of deformation lamellae (Fig. 2A) to dynamic recrystallization (Fig. 2B and C) is gradual in the section. The deformation lamellae are gently skewed (Fig. 2A) and abut against seams of dynamically recrystallized aggregates. The dynamic recrystallization occurs as thinner to wider seams of microcrystalline quartz aggregates, surrounding elongated domains of the precursory quartz with undulose extinction (Fig. 2B and C). The width of dynamically recrystallized seams ranges between 5 and 15 μm, whereas the width of the precursory quartz domains ranges between 20 and 150 μm.

Petrography and microthermometry of the fluid inclusion assemblages

In the studied chip, planar fluid inclusion assemblages were sought by lifting and lowering the stage of the microscope. The original growth zones (if they existed) were most probably obliterated by the deformation of the quartz lens, i.e., primary assemblages are not possible to define. The linear alignment of fluid inclusions is a result of their distribution along planes crosscutting the host quartz, i.e., on a phenomenological basis, the assemblages are FIPs, irrespective of their origin.

FIPs at high angles to the section (steep FIPs) appear as narrow stripes of inclusions, which sweep parallel to themselves as the microscope stage is being lowered or raised. Five distinct inclusion planes could be defined (Fig. 3). Inclusion planes at low angles to the section (low FIPs) appear as cloudy clusters of fluid inclusions (the second FIP in Fig. 3). In the studied chip, four steep FIPs and one low-angle FIP were identified. The studied FIPs terminate without crosscutting each other, most probably due to their trails being disturbed by the recrystallized zones. This in turn does not imply any temporal relationship between the recrystallization and the

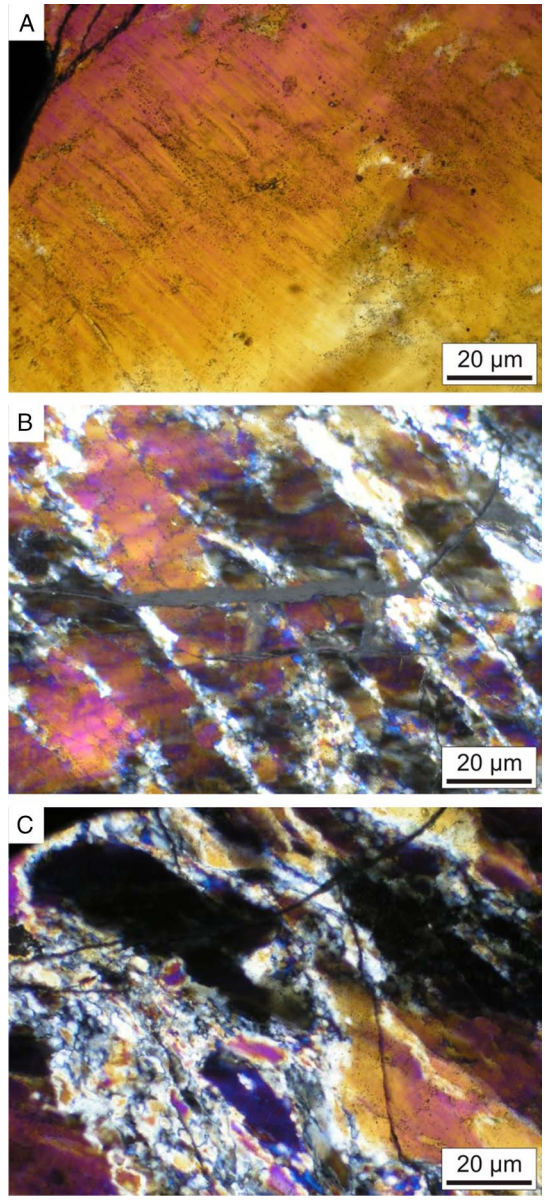

Fig. 2
Different textures of dynamic recrystallization inside the studied quartz sample. (A) Deformation lamellae (transmitted light, xN); (B) thinner (transmitted light, xN) to (C) wider seams of microcrystalline quartz aggregates, surrounding elongated domains of the precursory quartz with undulose extinction (transmitted light, xN)

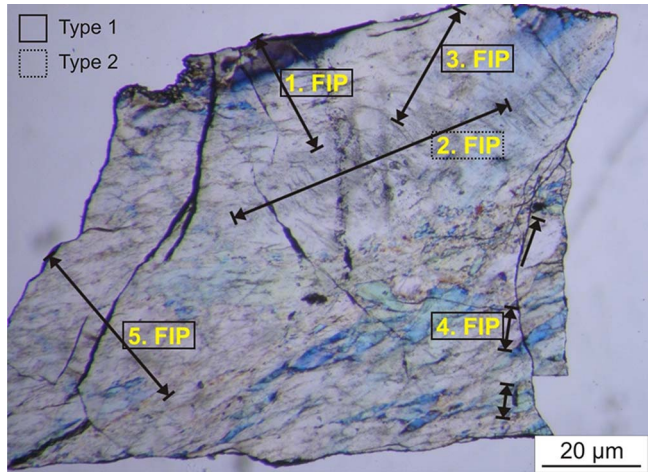

Fig. 3
Binocular transmitted light image of the studied chip, with the position of the studied FIPs

formation of the FIPs. Three inclusion types could be distinguished based on the volume ratios of the entrapped fluid and gas phases at room temperature. These groups are defined based on their petrographic appearance (shape, liquid/vapor ratio, and diameter), which means that each can possibly include several further fluid generations according to their microthermometric behavior.

Type 1 inclusions are two-phase, liquid–vapor inclusions with average "ϕ_{vapor}" (vapor–liquid ratios, "ϕ_{vapor}" = $A_{gaseous}/A_{total}$) between 0.2 and 0.25 and average diameters between 5 and 10 µm [note that "ϕ_{vapor}" values were assessed from areas (A) of certain fluid phases instead of volumes, hence we have marked them with quotation marks]. The inclusions display higher relief and resemble negative crystal forms (Figs 3 and 4B).

Type 2 inclusions are two-phase, liquid–vapor inclusions with average "ϕ_{vapor}" between 0.1 and 0.15 and average diameters between 3 and 6 µm. The inclusions are elongated and irregular in shape (Figs 3 and 4A).

Type 3 inclusions are small (around 1 µm in diameter) and are distributed along the deformation lamellae, but their appearance is basically different from those along the FIPs. They cannot be studied due to their small size.

SEM-based cathodoluminescence was applied to reveal crosscutting relationships between the FIPs and the recrystallized zones (Fig. 5), to see if they can be confidently defined by optical microscopy. One CL image was taken of an FIP containing Type 2 inclusions (the fourth FIP in Fig. 3), the trace of which along the studied chip is discontinuous, and is seemingly crosscut by the recrystallized zone (Fig. 5). The FIP, the narrow recrystallized domain and, the deformation lamellae in the domains of the precursory quartz are revealed on the CL image. Although the FIP becomes diffuse

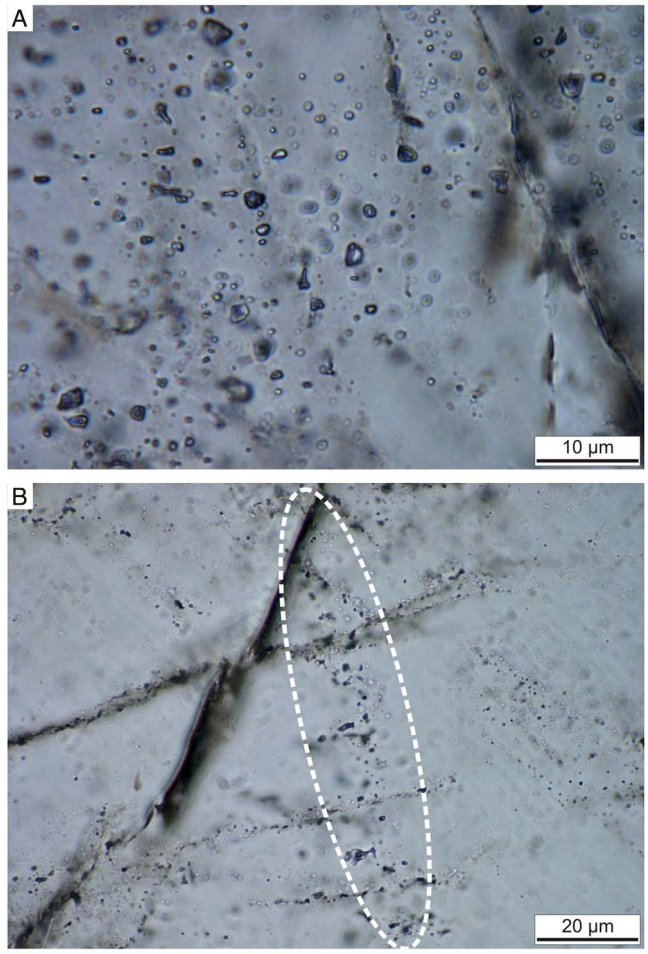

Fig. 4
(A) Type 1 inclusions are two-phase liquid–vapor inclusions with average vapor–liquid ratios between 0.2 and 0.25 and average diameters between 5 and 10 μm. Inclusions display higher relief and resemble negative crystal forms. (B) Type 2 inclusions are two-phase liquid–vapor inclusions with average vapor–liquid ratios between 0.1 and 0.15 and average diameters between 3 and 6 μm. Inclusions are elongated and irregular in shape. Dashed line marks the studied inclusion plane

along its section with the dynamically crystallized zone, the CL image suggests that the formation of the FIP postdates the dynamic recrystallization event (see inset in Fig. 5).

Three fluid generations can be distinguished based on microthermometric properties. The microthermometric properties of the entrapped fluids necessitate redefining the petrographic groups. For the sake of clarity, the petrographic classification is

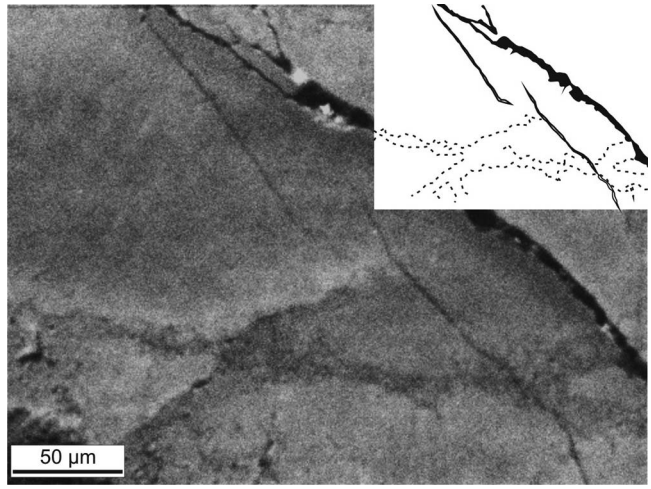

Fig. 5
CL image of an FIP (Type 1 inclusions) crosscutting a dynamically recrystallized zone of the quartz sample (dynamically recrystallized moat of quartz is displayed by darker zones in the CL image, delineated with dashed lines in the inset). The FIP markedly crosscut the recrystallized zone

mentioned for the groups defined by microthermometry. The inclusions of the third petrographic group are too small for microthermometric measurements, so they are not presented in the forthcoming groups defined by microthermometry.

Carbonic fluid inclusions are identical to the Type 1 inclusions. They homogenize to the liquid phase in a narrow range between 25.4 and 30.4 °C ($n = 35$) and have final melting temperatures between −57.2 and −56.2 °C (Fig. 6A and B). The final melting temperatures suggest a basically unary CO_2 fluid in the studied inclusions, which is in accordance with the low homogenization temperatures [$T_{crit}(CO_2) = 31.2$ °C]. Raman spectra of the inclusions indicate the presence of CO_2 in the inclusions, with a higher intensity peak at 1,386 and a lower one at 1,283 cm^{-1} (Fig. 7). Both peaks are shifted toward lower values, with respect to those published for pure CO_2 (1,388 and 1,285 cm^{-1}; Burke 2001 and references therein), which is in turn within the spectral resolution of the applied instrument.

The petrographically defined Type 2 inclusions contain two fluid generations, with different salinities (Table 1). The high-salinity fluid inclusions homogenize to the liquid phase between 75 and 123 °C ($n = 49$, Table 1, Fig. 6A). Final ice-melting occurs between −24.6 and −16.9 °C ($n = 49$, Fig. 6B). Based on an indefinite first melting temperature observation (ca. −50 °C), the inclusion fluid contains both NaCl and $CaCl_2$. However, due to the uncertain eutectic point observation, the fluid composition is considered as being representative of the H_2O–CaCl–NaCl system, which is constrained by the final melting temperatures lower than the eutectic temperature of the binary NaCl–H_2O system.

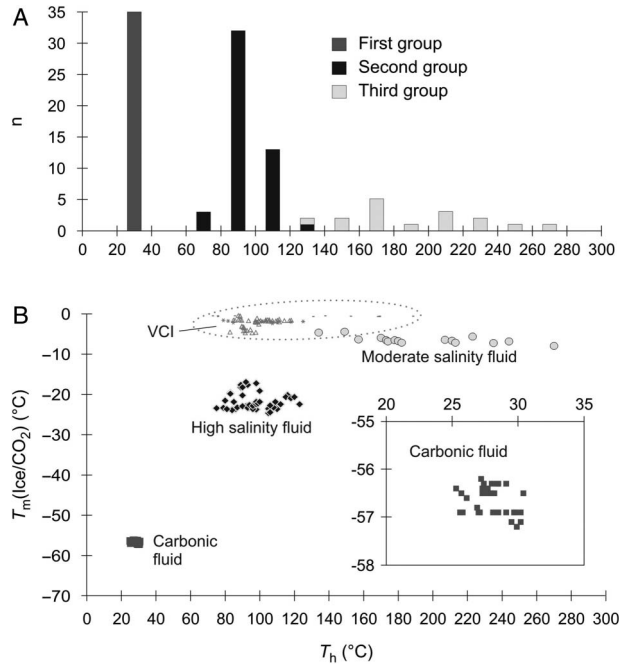

Fig. 6
(A) Histograms of measured T_h data. (B) T_h/T_m(ice) diagram of the studied inclusions. Groups are distinguished based on their microthermometric properties. VCI: vein carbonate hosted inclusions in the MZ (Dabi et al. 2011, 2013)

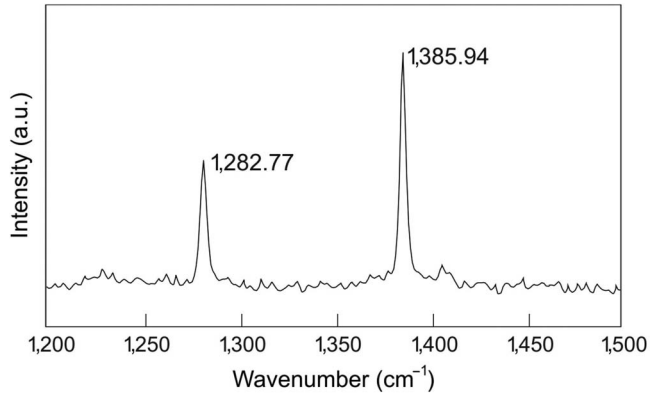

Fig. 7
Raman spectrum of the CO_2 inclusions entrapped in the studied sample

Table 1
Characteristics of petrographic types and microthermometric properties of the studied fluid inclusions

Petrographic types	Type 1	Type 2		Type 3
	$0.1 < \phi < 0.15$	$0.2 < \phi < 0.25$		
	Average diameters between 3 and 6 μm	Average diameters between 5 and 10 μm		Average diameter around 1 μm
	Negative crystal forms	Elongated and irregular in shape		Along the deformation lamellae
Microthermometric properties and composition	Carbonic	High salinity	Low salinity	No data
	$25.4 < T_h < 30.4$ °C	$75 < T_h < 123$ °C	$134 < T_h < 270$ °C	
	$-57.2 < T_m(CO_2) < -56.2$ °C	$-24.6 < T_m$(ice) < -16.9 °C	$-7.9 < T_m$(ice) < -4.4 °C	
	CO_2	H_2O–CaCl –NaCl	H_2O–NaCl (?)	

The moderate-salinity fluid has homogenization temperatures between 134 and 270 °C ($n = 49$), with a maximum frequency between 160 and 180 °C (Fig. 6A). Final ice-melting occurs between −7.9 and −4.4 °C ($n = 16$, Fig. 6B). Thus, the salinity of the fluid generation is between 7.2 and 11.7 mass% NaCl equivalent. First melting temperatures could not be observed due to the small size of inclusions. Petrographically, the fluid inclusions of the group cannot be distinguished from those with lower final melting temperatures (Type 2, based on phase ratios).

Discussion

Evolution of the quartz lens

Massive foliation-parallel metamorphic quartz lenses occur throughout the MZ, in the gneissic varieties of very different appearance and mineralogy. According to the latest concept of the internal build-up of the MZ at Ófalu, the northern part represents the lower structural unit of magmatic origin, whereas the southern part represents the higher unit comprised of metamorphic rocks of sedimentary origin (Koroknai 2009a). The magmatic origin of the northern unit is deduced from the study of M. Tóth et al. (2005), who investigated the morphology of zircons in samples mainly from the northern part of the Goldgrund valley. The sedimentary origin of the southern part is based on the presence of crystalline limestone bodies, and the presence of slate-like rocks ["Kövespatak Quartz Phyllite Formation," not

yet approved formation classification, proposed by Balla et al. (2009)], which are interpreted to be narrow sedimentary rock strips in the predominant gneisses (Gulácsi and Koroknai 2009).

However, the presence of massive metamorphic quartz veins is obvious in the northern part of the MZ, which is somewhat counterintuitive, considering the lower tendency of progressive metamorphism of quartzofeldspathic rocks to result in H_2O and quartz-producing reactions, at least in comparison with those of pelitic rocks (Bucher and Grapes 2011). Bons (2001) discusses the prevalence of massive metamorphic quartz veins at shallow crustal levels, where the temperature conditions and the resulting solubility of quartz necessitate unreasonably high amounts of fluid to precipitate the observed quartz volumes. To resolve this inconsistency, Bons (2001) suggested that a large volume of metamorphic fluids with high concentrations of dissolved SiO_2 accumulates at lower crustal levels, until a critical volume is reached. Then the fluid lens begins to travel upward in the crust as a mobile hydrofracture by simultaneous propagation at the upper tip and closure at the lower tip of the fluid-filled volume. The fluid-filled volume can ascend in this way in the crust at a speed on the order of several m/s. These "mobile hydrofractures" are arrested due to different causes, most of which are encountered at the brittle/ductile transition zone (Bons 2001). The detailed review of formation mechanism of the metamorphic quartz lenses is beyond the scope of this study. However, even if the quartz lenses are derived from an external source, according to the model of Bons (2001), the recrystallization texture suggests that the lens was present in the rock by the time ductile deformation ran its course.

Tullis et al. (2000) describe a sequence of features of progressive dynamic recrystallization of quartz from the Heavitree quartzite, from the Ruby Gap duplex, which forms a part of the internal ductile zones of the Alice Springs orogen in central Australia. The texture of the studied sample (i.e., the core–mantle structure with recrystallized moats around the domains of deformation lamellae) is similar to the Heavitree quartzite samples deformed with subgrain rotation recrystallization at greenschist conditions (dominant between 400 and 500 °C; Stipp et al. 2002). The domains of the deformation lamellae are remains of the quartz prior to the formation of recrystallized moats, a feature known as core–mantle structure (Passchier and Trouw 2005). Stipp et al. (2002) recognized an increase in recrystallized grains and the volume proportions of recrystallized material from 0% to 25% with increasing temperature in the regime of bulging recrystallization (BLG). Accordingly, they emphasize that core and mantle structures are not indicative of subgrain rotation exclusively but can be formed as a result of the lower temperature mechanism of BLG, i.e., at around 300 °C. However, the proper characterization of the dynamic recrystallization is not relevant to the inclusion petrography and is beyond the scope of this study. Based on whole rock Ar–Ar ages, Lelkes-Felvári et al. (2000) suggest 270 Ma as the minimum age of mylonitization of the MZ ultramylonites, i.e., the dynamic recrystallization features of the studied sample are considered to be no younger than 270 Ma.

Only one crosscutting segment of the recrystallized seams and the FIPs was studied with SEM CL (the fourth FIP in Fig. 3). Unfortunately, this apparatus is not optimal for studying quartz luminescence. However, the inclusion plane can be traced across the recrystallized seam in the CL image, which suggests that the precursory microcrack of the inclusion plane crosscut the recrystallized zone, i.e., recrystallization antedated the formation of the FIP. The conclusion is that the precursory microcracks of the inclusion planes decompose and become obscure where they crosscut recrystallized zones after healing. That is, inclusion plane sections with recrystallized zones in transmitted light cannot be used to determine their crosscutting relationships.

Interpretation of the fluid inclusion data

The presence of FIPs in the quartz lens indicates that the contained fluids are pervasive along the microcrack system held open by an active stress field (Lespinasse 1999), i.e., the FIPs are fossilized opening mode microfractures, perpendicular to the local σ_3 direction. Furthermore, FIPs are distributed systematically into suborthogonal directions around active faults, whereas their density (length/mm^2) logarithmically declines with distance from the causative fault (Faulkner et al. 2006, 2010; Mitchell and Faulkner 2009, 2012). On the whole, the tectonic origin of the fluid generations, as defined by the present microthermometric study, and their relation to fault activity are not out of question. However, the investigation of more samples from the study area is necessary for the verification of the involvement of fault activity.

The carbonic fluid

CO_2-rich fluids were not identified in the broader region of the study area, at least according to the best knowledge of the authors. This lack of recognizance of the CO_2 fluid generation becomes a striking feature if one considers that numerous thorough investigations have been carried out to reconstruct the paleohydrogeologic evolution of the MZ and that of the Mórágy Granite to the south (Szabó et al. 2003, 2008; Gatter and Török 2004; Poros et al. 2008; Dabi et al. 2009, 2011). In the studied sample, the in-sequence relationship of the CO_2-containing inclusion assemblage to the recrystallized quartz seams of the core–mantle structures could not be defined, i.e., the temporal relationship of the fluid flow event to the quartz recrystallization could not be identified. However, the lack of any remnants of CO_2 fluid flow in the Mórágy Granite suggests that (1) the fluid flow event occurred before the hydrogeologic evolution of the Mórágy Granite and that of the MZ metamorphic rocks became linked (Dabi et al. 2011), or (2) the CO_2-filled inclusion assemblage is the remnant of a local fluid flow event. As a third possibility (3), the possible fluid-modifying effect of recrystallization should be considered, which is of course only relevant in the case, where the CO_2 flow event antedated the recrystallization of the host quartz. Dabi et al. (2013) published a model of calcite-filled microcrack formation in the MZ, which presumes the segregation of a CO_2-rich fluid phase from a fluid with high CO_2 concentration during fault

activity contemporaneous with the Cretaceous dike emplacement in the area. Thus, it is also possible that (4) the studied inclusion assemblage was entrapped during the segregation of the high CO_2 fluid in the Cretaceous period of fault action. However, the same model suggests that the segregated CO_2 escaped the seismic microcrack system soon after its formation, accompanying the earthquake occurrence, while Mitchell and Faulkner (2012) suggest that fault action-related FIPs in quartz form in the interseismic period. Thus, the CO_2-filled inclusion assemblage was probably not entrapped during the fluid flow event that produced the Cretaceous calcite-filled microcrack generation in the study area (Dabi et al. 2013).

The presence of marble ("crystalline limestone") bodies in the MZ underscores the metamorphism of carbonate rocks in the study area. The marble contains tuff layers of several cm to 0.5 m thickness (Fülöp 1994). Although the description of the metamorphic assemblage of the marble has not yet been carried out, the coexistence of carbonate and silicate minerals in progressive metamorphism points to the passing-off of CO_2-producing metamorphic reactions (Bucher and Grapes 2011). The metamorphic origin of the CO_2-rich fluid explains its local occurrence, i.e., its confinement to the broader surroundings to the marble bodies.

The microthermometric behavior of the CO_2-rich fluid inclusions [$T_m(CO_2)$ between −57.2 and −56.2 °C] suggests high CO_2 concentrations, close to $X_{CO2} = 1$ of the entrapped fluid (Diamond 2003), which is in accordance with the occurrence of pure carbonic inclusions in shear zone-hosted quartz veins (Diamond et al. 2010 and references therein). Diamond et al. (2010) experimentally studied the effect of plastic deformation of the quartz host on the entrapped carbonic–aqueous inclusions. Their textural observations showed that the precursor inclusions tend to split apart during ductile deformation of the host quartz, where "dismembered" inclusions usually generate a cluster of inclusions consisting of a recognizable relict of the precursor, surrounded by smaller neonate inclusions. It was also demonstrated that the neonates are distributed into planar clusters along crystallographic planes of the host quartz. The crowd of small fluid inclusions distributed along the quartz laminae could possibly be the equivalents of the experimentally produced neonates, whereas the CO_2-filled inclusions are possibly the equivalents of the relict inclusions in the experiments of Tarantola et al. (2010). Diamond et al. (2010) demonstrated that the densities of the inclusions changed due to the volume expansion of the inclusions (by being connected to the newly formed neonates), whereas the composition of the relict and neonate inclusions did not change. Accordingly, they suggest that the prevalence of pure carbonic inclusions in shear zones is due to phase exsolution (and segregation?) of the carbonic and aqueous components, if quartz deformation occurs with similar mechanisms at lower crustal depths than those attained during their experiments, closer to the miscibility boundary of the specific CO_2–H_2O–NaCl fluid system.

On the whole, most probably, the fluid was entrapped in the CO_2-containing fluid inclusions as a carbonic aqueous fluid generation, which lost its H_2O component during subsequent plastic deformation of the host, due to the higher mobility of H_2O in quartz (Diamond et al. 2010). The H_2O component is probably entrapped along the

swarms of minute (<1 μm) inclusions distributed along the deformation lamellae of the host quartz (the petrographically distinguished Type 3 group, Table 1). That is, the entrapment of the fluid generation antedated quartz recrystallization.

The high-salinity fluids

One inclusion plane (the fourth FIP in Fig. 3) containing the high-salinity fluid postdates the recrystallization, according to the CL image. The high-salinity fluids (homogenization temperatures between 75 and 123 °C and final ice-melting temperatures between −24.6 and −16.9 °C) are similar to those identified by Szabó et al. (2003) in the vein calcite of quartz–calcite and dolomite–calcite veins of the Mórágy Granite to the south. These fluids were considered by Szabó et al. (2003) as being related to the very low salinity [T_m(ice) as high as −0.2 °C] fluids of crosscutting veins in the same study area, together being representative of the hydrothermal phase of granite evolution. Based on its salinity (as implied by the measured final melting temperatures), the fluid can also be related to those identified in the FIPs of the rock-forming quartz of the Mórágy Granite [T_m(ice) between −25 and −19 °C; Poros et al. 2008]. However, homogenization temperatures indicate a higher fluid temperature in the case of the Mórágy Granite (T_h between 175 and 255 °C; Poros et al. 2008), while the homogenization temperatures entrapped in the vein calcites crosscutting the granite (T_h between 90 and 160 °C; Fig. 94 in Szabó et al. 2003) are similar to those entrapped in the metamorphic quartz. Fintor et al. (2008) identified high-salinity fluids [T_m(ice) between −27.4 and −18.8 °C, with T_h between 71 and 182 °C] in inclusions entrapped in vein-forming quartz and carbonate from the Baksa metamorphic complex, 40 km southwest of this study area. Fintor et al. (2008) convincingly propose that the high-salinity fluid was extraformational sedimentary brine, or that the dissolved components were acquired by the fluid during its interaction with the above-lying evaporitic strata (most probably those of the Triassic Hetvehely Dolomite Formation). Assuming that the MZ metamorphic rocks were covered by similar sediments during the Late Paleozoic–Mesozoic until the early to middle period of the Alpine tectonic cycle (Császár 2003), a similar sedimentary origin of the high-salinity fluid is also possible in the case of the high-salinity inclusion fluids of the MZ. In this case, it is plausible to assume that the temperature of fluids was governed by the local geothermal gradient, which suggests a depth of the MZ metamorphic rocks between 2.5 and 4 km (by applying an average geothermal gradient of 30 °C). Poros et al. (2008) identified the fluid in FIPs with NE–SW and NW–SE strike, i.e., in suborthogonal sets, which they interpreted as a result of stress perturbation. However, since the publication of the study of Poros et al. (2008), that of Mitchell and Faulkner (2009), demonstrated that FIPs containing the high-salinity fluids are distributed into suborthogonal sets around active faults, i.e., the high-salinity fluid is possibly related to an active period of either of the fault generations crosscutting the Mórágy Granite (see Fig. 9 in Maros et al. 2009).

On the other hand, the high-salinity fluid identified by Poros et al. (2008) has a higher homogenization temperature range than that defined by our measurements, which do not rule out that the two fluids are consistent with a common origin. Their common origin necessitates different pressure and temperature of the same fluid in the two formations.

On the whole, the high-salinity fluid is most probably related to a regional fluid flow event derived from the above-lying sedimentary sequences. The presence of the fluid generation in suborthogonal sets in the Mórágy Granite (Poros 2007) suggests that the fluid flow is related to fault action (Mitchell and Faulkner 2009). The lack of similar fluids as primary fluids in veins, or secondary assemblages crosscutting veins in the MZ, suggests that the flow event antedated the period of vein formation (Dabi et al. 2011).

The moderate-salinity fluid

The moderate-salinity fluid (final ice-melting temperatures between −7.9 and −4.4 °C, and homogenization temperatures between 134 and 270 °C, with a maximum frequency between 160 and 180 °C; Fig. R5B) was not identified by earlier paleofluid studies of the MZ, i.e., it is not present in the vein system crosscutting the MZ, neither as primary nor as secondary trails. This suggests that the fluid flow antedated the beginning of the vein-producing brittle deformation history of the MZ, which is in turn not older than Triassic (Dabi et al. 2011). Similar data are displayed in the report of Szabó et al. (2003), without being distinguished as a separate subgroup. According to the interpretation of Szabó et al. (2003), the entire set of the measured microthermometric data indicates a continuous trend of hydrothermal undilution. This interpretation is, however, disproved by the microthermometric data and their interpretation by subsequent studies (Poros et al. 2008; Szabó et al. 2008; Dabi et al. 2011, 2013), which have demonstrated that the moderate-salinity fluids are related to the Cretaceous dike emplacement in the region. Poros et al. (2008) have measured very similar homogenization temperatures in a NE–SW subset of FIPs, with T_h between 103 and 116 °C and T_m(ice) between −8.2 and −5.2 °C, which they joined to a wider but overlapping subset of their data, and considered as being representative of a Late Cretaceous, undiluting fluid system. However, in the case if the two fluids [those defined by Poros et al. (2008) and that defined in this study] were entrapped during the same flow event, the Cretaceous age of the flow event and thus its relationship to the Cretaceous dike emplacement are questionable.

The relative timing of the moderate-salinity fluid flow event was not investigated with CL. However, considering the modifying effect of recrystallization on the fluid compositions and the likelihood of H_2O loss from inclusions during the recrystallization of the host quartz (Diamond et al. 2010; Tarantola et al. 2010), the relatively uniform salinities of the entrapped fluids suggest that the inclusions were entrapped following recrystallization.

Timing of the fluid flow events

Dabi et al. (2009, 2011) defined seven subsequent vein-filling mineral generations in the MZ metamorphic complex, the youngest of which is interpreted to be related to the Triassic carbonate sediments in the area, based on its stable isotope compositions (Dabi et al. 2011). The defined fluid generations were not identified in any of the vein generations crosscutting the MZ metamorphic rocks (Dabi et al. 2009, 2011), which suggest that the flow events antedated the Mesozoic brittle deformation of the MZ. This in turn contradicts the relationship of the high-salinity fluid generation to the Triassic evaporite sequences, as suggested by Fintor et al. (2008). The lack of vein minerals containing the defined fluid generations in primary or secondary assemblages suggests that the FIPs were formed during the early stage of the uplift history of the metamorphic belt (Császár 2003), during which the macroscopic fracture formation was not favored. However, the refinement of timing of fluid flow events (including relative timing) necessitates further investigation of the FIPs contained in metamorphic quartz lenses from around the MZ metamorphic complex.

The entrapment of the carbonic fluid inclusions antedated the recrystallization of the studied quartz lens, according to the interpretation that the CO_2 was concentrated in the inclusions as a result of recrystallization-related H_2O loss. The small (Type 3) inclusions along the deformation lamellae of the host quartz are most probably analogous to the neonate inclusions formed during the experiment of Tarantola et al. (2010) and Diamond et al. (2010), and probably contain the H_2O component of the CO_2-containing inclusions. The relatively narrow range of salinities in the Type 2 inclusions (the moderate- and high-salinity fluids) suggests that they were not modified by the recrystallization of the host mineral, and postdate recrystallization. In the case of the high-salinity fluid containing FIPs, the timing was also constrained by SEM CL.

Conclusions

Fluid inclusion petrography and microthermometry of one single, unoriented metamorphic quartz sample resulted in new information about the paleofluid evolution of the MZ metamorphic complex. FIP studies had been carried out by previous authors in the Mórágy Granite to the south (Poros et al. 2008; Szabó et al. 2008); thus it is plausible to examine similar formations in the MZ rocks if present, to obtain a deeper understanding of the regional paleofluid evolution. This study should be considered as a tryout of the rock-forming quartz lenses in the MZ to determine whether they are amenable to similar studies. Our results indicate that the interpretation of the FIP petrography is rendered problematic due to the mylonitization-related recrystallization of the quartz lens, which is probably a ubiquitous feature in the MZ.

The gathered microthermometric data allow the definition of three fluid generations, none of which have been recognized in the study area in earlier paleofluid

studies. The lack of presence of the fluids defined in this study as primary or secondary assemblages in the crosscutting vein systems of the MZ suggests that their occurrence preceded the main period of brittle deformation (vein formation) of the MZ metamorphic complex (between Triassic and Cretaceous; Dabi et al. 2011). The inclusions containing the carbonic fluid were presumably modified by the ductile deformation of the host quartz, leaving a high X_{CO2} fluid in the relict inclusions. The high-salinity fluid can be related to a regional fluid flow event and considered as being derived from evaporitic sequences of the above-lying sedimentary pile (Fintor et al. 2008). A low-salinity fluid is also identified, which is probably related to the fluids mentioned by Poros et al. (2008). However, its relationship to the Cretaceous hydrothermal activity in the Mórágy Granite, as assumed by Poros et al. (2008), is questionable.

Acknowledgements

The authors would like to thank the anonymous reviewers, whose comments helped greatly in improving the manuscript.

References

Balla, Z., G. Császár, B. Koroknai 2009: The NW boundary of the Mecsekalja Zone. – In: Balla, Z., L. Gyalog (Eds): Geology of the North-eastern Part of the Mórágy Block. Geological Institute of Hungary, Budapest, pp. 147–148.

Bons, P.D. 2001: The formation of large quartz veins by rapid ascent of fluids in mobile hydrofractures. – Tectonophysics, 336, pp. 1–17.

Bucher, K., R. Grapes 2011: Petrogenesis of Metamorphic Rocks. – Springer-Verlag, Berlin, Heidelberg, 428 p.

Burke, E.A.J. 2001: Raman microspectrometry of fluid inclusions. – Lithos, 55, pp. 139–158.

Császár, G. 2003: Alpine burial history of the Mórágy Block and its environs. – Annual Report of the Geological Institute of Hungary, 2003, pp. 395–406.

Dabi, G., F. Schubert, T.M. Tóth 2009: Carbonate veins of different texture and their role in reconstructing fracture cementation. – Bulletin of the Hungarian Geological Society, 139, pp. 3–20.

Dabi, G., Z. Siklósy, F. Schubert, B. Bajnóczi, T.M. Tóth 2011: The relevance of vein texture in understanding the past hydraulic behaviour of a crystalline rock mass: Reconstruction of the palaeohydrology of the Mecsekalja Zone, South Hungary. – Geofluids, 11, pp. 309–327.

Dabi, G., B. Bajnóczi, F. Schubert, T.M. Tóth 2013: The origin and role of a calcite-filled microcrack generation in a metamorphic crystalline complex: The characterization of a fossilised seismic permeability system. – Tectonophysics, 608, pp. 792–803.

Diamond, L.W. 2003: Systematics of H_2O inclusions. – In: Samson, I., A. Anderson, D. Marshall (Eds): Fluid Inclusions: Analysis and Interpretation. Mineralogical Association of Canada, Québec, pp. 101–158.

Diamond, L.W., A. Tarantola, H. Stünitz 2010: Modification of fluid inclusions in quartz by deviatoric stress. II: Experimentally induced changes in inclusion volume and composition. – Contributions to Mineralogy and Petrology, 160, pp. 845–864.

Faulkner, D.R., T.M. Mitchell, D. Healy, M.J. Heap 2006: Slip on 'weak' faults by the rotation of regional stress in the fracture damage zone. – Nature, 444, pp. 922–925.

Faulkner, D.R., C.A.L. Jackson, R.J. Lunn, R.W. Schlische, Z.K. Shipton, C.A.J. Wibberley, M.O. Withjack 2010: A review of recent developments concerning the structure, mechanics and fluid flow properties of fault zones. – Journal of Structural Geology, 32, pp. 1557–1575.

Fintor, K., F. Schubert, T.M. Tóth 2008: Indication of hypersaline palaeofluid migration in the fracture system of the Baksa Gneiss Complex. – Bulletin of the Hungarian Geological Society, 138/3, pp. 257–278.

Fülöp, J. 1994: Magyarország geológiája – Pelozoikum II (Geology of Hungary – Palaeozoic II). – Akadémiai Kiadó, Budapest, 447 p. (in Hungarian)

Gatter, I., K. Török 2004: Mineralogical notes and fluid inclusion studies on quartz-feldspar granite pegmatites and quartz veins from Mórágy and Erdősmecske granitoid, S-Hungary. – Acta Mineralogica-Petrographica, Szeged, 45/1, pp. 39–48.

Goldstein, R.H., T.J. Reynolds 1994: Systematics of fluid inclusions in diagenetic minerals. – SEPM Short Course Notes, 31, 199 p.

Gulácsi, Z., B. Koroknai 2009: Lower Palaeozoic, Ófalu Group. – In: Balla, Z., L. Gyalog (Eds): Geology of the North-eastern Part of the Mórágy Block. Geological Institute of Hungary, Budapest, pp. 48–57.

Koroknai, B. 2009a: Structural pattern of the Mecsekalja Zone. – In: Balla, Z., L. Gyalog (Eds): Geology of the North-eastern Part of the Mórágy Block. Geological Institute of Hungary, Budapest, pp. 146–147.

Koroknai, B. 2009b: Hydrothermal phenomena in connection with alkali volcanites. – In: Balla, Z., L. Gyalog (Eds): Geology of the North-eastern Part of the Mórágy Block. Geological Institute of Hungary, Budapest, pp. 79–81.

Lelkes-Felvári, G.Y., P. Árkai, W. Frank, G. Nagy 2000: Late Variscan ultramylonite from the Mórágy Hills, SE Mecsek Mts., Hungary. – Acta Geologica Hungarica, 43, pp. 65–84.

Lespinasse, M. 1999: Are fluid inclusion planes useful in structural geology? – Journal of Structural Geology, 21, pp. 1237–1243.

Maros, G.Y., B. Koroknai, K. Palotás, L. Fodor, A. Dudko, M. Forián-Szabó, L. Zilahi-Sebess, E. Bán-Győri 2004: Tectonic analysis and structural evolution of the north-eastern Mórágy-Block. – Annual Report of the Geological Institute of Hungary, 2003, pp. 361–369.

Maros, G.Y., B. Koroknai, K. Palotás, B. Musitz, J. Füri, J. Borsody, P. Kovács-Pálffy, P. Kónya, I. Viczián, K. Balogh, Z. Pécskay 2009: Brittle fault zones in the Mórágy Granite (South Transdanubia): New structural and K–Ar data. – Annual Report of the Geological Institute of Hungary, 2009, pp. 91–112.

Mitchell, T.M., D.R. Faulkner 2009: The nature and origin of off-fault damage surrounding strike-slip fault zones with a wide range of displacements: A field study from the Atacama fault system, northern Chile. – Journal of Structural Geology, 31, pp. 802–816.

Mitchell, T.M., D.R. Faulkner 2012: Towards quantifying the matrix permeability of fault damage zones in low porosity rocks. – Earth and Planetary Science Letters, 339–340, pp. 24–31.

Passchier, C.W., R.A.J. Trouw 2005: Microtectonics. – Springer-Verlag, Berlin, Heidelberg, New York, 366 p.

Paterson, M.S., T.-F. Wong 2005: Experimental Rock Deformation – The Brittle Field. – Springer-Verlag, New York, 347 p.

Poros, Z.S. 2007: A Mórágyi Gránit paleo-fluidumáramlás rekonstrukciója és repedésrendszereinek vizsgálata Bátaapáti fúrásokban (Application of fluid inclusion planes for reconstruction of fracture development and palaeofluid flow patterns in the Mórágy Granite Formation (Bátaapáti, Mecsek Mts.)). – MSc Thesis, Eötvös Loránd University, Budapest, 115 p. (in Hungarian)

Poros, Z.S., F. Molnár, B. Koroknai, M. Lespinasse, G.Y. Maros, Z.S. Benkó 2008: Application of studies on fluid inclusion planes and fracture systems in the reconstruction of the fracturing history of granitoid rocks III: Results of studies in drill cores from the radioactive waste depository site at Bátaapáti (Üveghuta). – Bulletin of the Hungarian Geological Society, 138, pp. 361–383.

Stipp, M., H. Stünitz, R. Heilbronner, S.M. Schmid 2002: The eastern Tonale fault zone: A 'natural laboratory' for crystal plastic deformation of quartz over a temperature range from 250 to 700 °C. – Journal of Structural Geology, 24, pp. 1861–1884.

Szabó, B., Z.S. Benkó, F. Molnár, M. Lespinasse 2008: The application of studies on fluid inclusion planes and fracture systems in the reconstruction of fracturing history of granitoid rocks II: Fracture systems of the Mórágy Granite. – Bulletin of the Hungarian Geological Society, 138/3, pp. 247–256.

Szabó, C.S., K. Gál-Sólymos, A. Fall 2003: Karbonátos repedéskitöltés vizsgálatok Üveghuta környékén mélyített fúrások granitoid kőzetein – Kis és közepes radioaktivitású erőművi hulladékok végleges elhelyezése. Telephelykutatás Üveghuta körzetében (Investigation of carbonate veins from core samples drilled in the Granitoid rocks around Üveghuta – Final disposal of low- and intermediate-level radioactive waste. Site investigation in the district around Üveghuta). – Manuscript, Geological Institute of Hungary, Budapest, 110 p. (in Hungarian)

Tarantola, A., L.W. Diamond, H. Stünitz 2010: Modification of fluid inclusions in quartz by deviatoric stress I: Experimentally induced changes in inclusion shapes and microstructures. – Contributions to Mineralogy and Petrology, 160, pp. 825–843.

Tóth, T.M., G. Kovács, F. Schubert, V. Dályai 2005: Origin and deformation history of the Ófalu "migmatite". – Bulletin of the Hungarian Geological Society, 135, pp. 331–352.

Tullis, J., H. Stünitz, C. Teyssier, R. Heilbronner 2000: Deformation microstructures in quartzo-feldspathic rocks. – Journal of the Virtual Explorer, 2, http://www.virtualexplorer.com.au/article/microstructures-quartzo-feldspathic-rocks.